

Impact of TRMM SSTs on a Climate-Scale SST Analysis

RICHARD W. REYNOLDS

NOAA/NESDIS/National Climatic Data Center, Asheville, North Carolina

CHELLE L. GENTEMANN AND FRANK WENTZ

Remote Sensing Systems, Santa Rosa, California

(Manuscript received 15 July 2003, in final form 15 January 2004)

ABSTRACT

Prior efforts have produced a sea surface temperature (SST) optimum interpolation (OI) analysis that is widely used, especially for climate purposes. The analysis uses in situ (ship and buoy) and infrared (IR) satellite data from the Advanced Very High Resolution Radiometer (AVHRR). Beginning in December 1997, "microwave" SSTs became available from the Tropical Rainfall Measuring Mission (TRMM) satellite Microwave Imager (TMI). Microwave SSTs have a significant coverage advantage over "IR" SSTs because microwave SSTs can be retrieved in cloud-covered regions while IR SSTs cannot. However, microwave SSTs are at a much lower spatial resolution than the IR SSTs.

In this study, the impact of SSTs derived from TMI was tested from the perspective of the OI analysis. Six different versions of the OI were produced weekly from 10 December 1997 to 1 January 2003 using different combinations of AVHRR and TMI data and including versions with and without a bias correction of the satellite data. To make the results more objective, 20% of the buoys were randomly selected and the SSTs from these buoys were withheld from the OI for independent verification.

The results of the intercomparisons show that both AVHRR and TMI data have biases that must be corrected for climate studies. These biases change with time as physical properties of the atmosphere change and as satellite instruments and the orbits of the satellites, themselves, change. It is critical to monitor differences between satellite and other products to quickly diagnose any of these changes.

For the OI analyses *with* bias correction, it is difficult using the withheld buoys to clearly demonstrate that there is a significant advantage in adding TMI data. The advantage of TMI data is clearly shown in the OI analyses *without* bias correction. Because IR and microwave satellite algorithms are affected by different sources of error, biases may tend to cancel when both TMI and AVHRR data are used in the OI. Bias corrections cannot be made in regions where there are no in situ data. In these regions, the results of the analyses without bias corrections apply. Because there are areas of the ocean with limited in situ data and restricted AVHRR coverage due to cloud cover, the use of both TMI and AVHRR should improve the accuracy of the analysis in these regions. In addition, the use of more than one satellite product is helpful in diagnosing problems in these products.

1. Introduction

Reynolds and Smith (1994) and Reynolds et al. (2002) produced an optimum interpolation (OI) sea surface temperature (SST) analysis that is widely used for weather forecasting, climate monitoring, climate prediction, and both oceanographic and atmospheric research, as well as specifying the surface boundary condition for atmospheric analysis and reanalysis. The analyses appear in many publications and are available to any user via the Internet. The analysis is produced weekly on a 1° spatial grid and uses both in situ and satellite data.

When the OI analysis was originally developed there was only one satellite instrument available to operationally measure SST. This instrument was the infrared (IR) Advanced Very High Resolution Radiometer (AVHRR), which was one of the instruments on the National Oceanic and Atmospheric Administration (NOAA) Polar-orbiting Operational Environmental Satellites. In roughly the last decade, new infrared sensors, such as the Moderate Resolution Imaging Spectroradiometer (MODIS), have become available on other satellites, but have yet to become assimilated into the OI analysis. Beginning in December 1997, SSTs began to be available on the Tropical Rainfall Measuring Mission (TRMM) satellite, which is a joint mission between the National Aeronautics and Space Administration (NASA) and the National Space Development Agency (NASDA) of Japan. Because of its low-inclination orbit,

Corresponding author address: Dr. Richard W. Reynolds, NOAA/National Climatic Data Center, 151 Patton Avenue, Asheville, NC 28801.
E-mail: Richard.W.Reynolds@noaa.gov

the TRMM Microwave Imager (TMI) produces SSTs from roughly 38°S to 38°N. Additional microwave instruments have become available in late 2002 and more are planned. SSTs from microwave instruments have lower spatial resolution than from IR instruments. However, microwave instruments are able to retrieve SSTs in cloud-covered regions where IR instruments cannot. Retrievals in cloud-covered regions are a big advantage of microwave instruments. For a relatively low spatial resolution analysis like the OI, the lower resolution of a microwave instrument is not important.

Stammer et al. (2003) compared the weekly OI and TMI SSTs. In this comparison, TMI retrievals were averaged onto a weekly 1° grid. They concluded that TMI would add significant value to products based on IR instruments alone. However, Stammer et al. did not address the problem of how to merge TMI with another analysis to ensure that a combined analysis would be consistent in periods before TMI was available and at high latitudes where TMI cannot retrieve SSTs.

Our purpose is to study the usefulness of TMI from the perspective of the OI analysis. This is, of course, a somewhat limited goal because higher resolutions are now possible in space and time because of the increasing number of SST-measuring satellite missions. However, we believe this comparison is of interest for climate-scale studies of SSTs. In the sections that follow, we first briefly discuss the present OI analysis and its input data. We then review the TMI algorithm and the changes in the algorithm that have led to the present version. Next we discuss our procedures for the comparison and finally present our results and conclusions.

2. Data and analyses

a. OI input data

The in situ SST data are obtained from observations from ships and buoys (both moored and drifting). Selected SST observations can be very accurate (see Kent et al. 1993, 1999). However, typical rms errors of individual observations from ships (e.g., see Reynolds and Smith 1994) are larger than 1°C. SST observations from drifting and moored buoys were first used in the late 1970s and became more plentiful beginning in 1985. Although the accuracy of the buoy SST observations varies, the random error is usually smaller than 0.5°C and, thus, is smaller than ship error. In addition, typical depths of the measurements are roughly 0.5 m, rather than the 1-m-and-deeper measurements from ships.

In late 1981, AVHRR satellite retrievals improved the data coverage over that of in situ observations alone (see, e.g., Reynolds and Smith 1994). Because clouds obstruct AVHRR retrievals, the biggest challenge in retrieving IR SST is to eliminate cloud-contaminated retrievals. The algorithms are “tuned” by regression against quality-controlled buoy data using the multi-channel SST technique of McClain et al. (1985). This

procedure converts the retrieval of the temperature of the “skin” [1 mm in depth (Fairall et al. 1996) or less (Donlon et al. 2002)] to a “bulk” (roughly 0.5 m in depth) SST. The algorithm is usually tuned and applied separately for daytime and nighttime using two IR channels during the day and three at night (May et al. 1998). The algorithms are computed globally and are not a function of position or time. Negative satellite SST biases usually indicate cloud or atmospheric aerosol contamination (see Reynolds et al. 1989; Reynolds 1993). In the results presented here the AVHRR data was processed by the U.S. Navy as described in May et al. (1998).

b. OI analysis

Optimum interpolation was developed by Gandin (1963) as an objective analysis method for irregularly spaced data. At each analysis grid point, the analysis method objectively determines a series of weights for each of the data increments. The data increment is defined as the difference between each observation and the analysis first guess interpolated spatially to the position of the observation. Reynolds and Smith (1994) use the previous week’s analysis as the first guess. The analysis is optimal if all the error covariances and the data signal-to-noise ratios are known perfectly. Because these parameters are only approximately known, the OI is only approximately optimized. The OI analysis is computed weekly on a 1° latitude by 1° longitude grid using AVHRR satellite and in situ data discussed previously. The OI method assumes that the data do not contain long-term biases (e.g., see Lorenc 1981). Because satellite biases occur in our period of interest, a preliminary step using Poisson’s equation is carried out to remove satellite biases relative to in situ data before the OI analysis is begun. This method adjusts any large-scale satellite biases and gradients relative to the in situ data. In the OI procedure, various error statistics are assigned that are a function of latitude and longitude. (The average zonal and meridional spatially correlated error e -folding scales are 615 and 850 km, respectively. The average guess error is 0.3°C. The average data errors are 1.3°, 0.5°, 0.5°, and 0.3°C for ships, buoys, daytime AVHRR, and nighttime AVHRR, respectively.) For more details see Reynolds and Smith (1994) and Reynolds et al. (2002).

c. TMI data

The TRMM satellite has an orbital inclination of 35° and an altitude of 350 km (raised to 402 km in August 2001). This yields coverage from roughly 38°S to 38°N. Almost complete coverage within these latitudinal bounds is achieved every 2 days. The equatorial orbit precesses with a period of 23 days, to better sample the diurnal cycle. The TMI is essentially a Special Sensor Microwave Imager (SSM/I) with an additional 10.7-GHz

channel. The 1-m reflector results in an elliptical footprint of $34 \text{ km} \times 46 \text{ km}$ at 10.7 GHz.

The Remote Sensing Systems TMI SST algorithm is physically based, relying primarily on the 10.7-GHz channel. SST retrieval is one parameter out of a complete ocean suite that is produced (Wentz and Meissner 1999). Algorithm coefficients were developed using a complete radiative transfer model. A large volume of environmental scenes were generated using 42 195 radiosonde profiles, five cloud models, randomly varied SSTs, randomly varied wind speed, and randomly varied wind direction. Simulated brightness temperatures were generated using the radiative transfer model, then coefficients were derived for a multiple linear regression algorithm. At 10.7 GHz, the brightness temperatures have a nonlinear response to SST and wind speed. As the response is not highly nonlinear, it can be accounted for by a two-stage regression. Algorithm coefficients were determined for 56 sets of different wind–SST regimes. The baseline algorithm produced a wind and SST, which were used to narrow the retrievals into four specific wind–SST regimes. On this smaller scale, the brightness temperature response is fairly linear. The main source of error for this method of retrieval is wind speed/direction effects on the emissivity. To account for this, National Centers for Environmental Prediction (NCEP) 10-m wind directions were used as an input to the algorithm to account for directional effect, while wind speed was calculated directly using the TMI brightness temperatures. The rms error in the NCEP directions is about 20° on a global basis. For wind speeds below 8 m s^{-1} , the directional signal in the 11-GHz brightness temperature is very small, having an rms variation of 0.2 K or less. In this case, the use of NCEP wind directions introduces negligible error. However, the directional signal increases at higher winds. For example, for winds near 15 m s^{-1} , a 20° error in the NCEP direction translates into a $0.5^\circ\text{--}1^\circ\text{C}$ error in the SST retrieval.

The largest errors in the TMI SST retrievals occur near land and at high wind speeds. In addition, errors are caused by engineering problems with the main reflector and the onboard satellite attitude control system. Near land, sidelobe contamination will result in a positive bias of the SST retrievals. For this reason, the algorithm is not run within 50 km of land. However, some contamination is still present. At high wind speeds, greater than 12 m s^{-1} , increased uncertainty in determination of the correct surface emissivity will result in increased uncertainty in the TMI SST retrievals. As mentioned in Wentz et al. (2001), a problem with TMI's main reflector adds a bias to all retrievals. A correction has been developed and is applied to brightness temperatures before processing data. Finally, the SST retrieval algorithm is extremely sensitive to incidence angles and errors in the calculation of incidence angles propagate into the SST retrieval. Careful corrections for errors in the onboard calculation of incidence

angles are applied to the TMI retrievals to minimize the impact on SSTs.

3. Procedure

For this study we use the OI version 2 (OI.v2) analysis discussed in Reynolds et al. (2002). This is a replacement of the OI version 1 analysis discussed in Reynolds and Smith (1994). The OI.v2 analysis has a modest improvement in the bias correction because of the addition of more in situ data and uses an improved climatological sea ice–to-SST conversion algorithm that better fits the SST data.

In the analysis procedure all observations are reduced to superobservations, which are defined as averages over 1° squares. The averaging is computed for ship and buoy data by individual call sign or identification (ID) number. The superobservations are also computed for each type of satellite data: TMI, and daytime and nighttime AVHRR. This of course limits the maximum spatial grid resolution to 1° . The actual resolution is coarser due to the assumed OI error correlation scales.

The division into daytime and nighttime categories is useful for AVHRR because the algorithm and cloud detection routines differ. AVHRR daytime cloud detection algorithms and SST equations are used when the solar zenith angle is less than 75° . Nighttime cloud detection algorithms and SST equations are used for solar zenith angles greater than 90° if the channel-2 (a visible channel) reflectance is less than 1%. For solar zenith angles between 75° and 90° , nighttime cloud detection and SST equations are used if the channel-2 reflectance is less than 1.8% (May et al. 1998).

We initially divided the TMI data into day and night categories. The division was defined by local time of the retrieval. Day is defined by times between 0800 and 2000 local time while night was the remainder. However, the analyzed results tended to be noisy at higher latitudes due to sparse sampling as discussed at the beginning of the next section. Thus, the TMI product used in the OI analyses was a combined product in which day- and nighttime data were averaged together based on the total number of observations. (In the OI, the TMI data errors were assumed equal to the nighttime AVHRR errors.)

There are diurnal signals in the SST data. However, they cannot be resolved in a weekly analysis and are treated as noise here. In most regions of the ocean the diurnal signals are small. However, they can reach amplitudes of 3°C in the western tropical Pacific as shown in the last figure of Reynolds et al. (2001). However, as shown there, the amplitude peaks at 1400 to 1500 local time and does not occur every day. Either AVHRR or TMI coverage is not adequate even ignoring cloud cover to sample the entire tropical ocean daily. Furthermore, the precession of the TMI equatorial crossing further complicates sampling of the peak diurnal warming. The AVHRR *NOAA-14* and *NOAA-16* instruments were designed to cross the equator daily at 1400 local

time. However, as discussed below, the orbit of *NOAA-14* decayed so that near the end of its lifetime the equatorial crossing was closer to 1800 local time. Thus, even a high-resolution SST analysis would require an embedded model to get the diurnal signals correct.

We computed six different OI.v2 analyses, which can be divided into two groups. One group consists of analyses with the satellite bias correction step; the second group consists of analyses without the bias correction step. All analyses use the same in situ and sea ice data. In each group there are three analyses that will use different satellite data. The first analysis uses only AVHRR satellite data (henceforth, AVHRR only). The second analysis uses only TMI satellite data (henceforth, TMI only). The third combines both AVHRR and TMI data (henceforth, TMI + AVHRR). In the analyses, TMI, the daytime AVHRR, and nighttime AVHRR data are separately corrected in the bias correction step using the same in situ data.

To allow quantitative estimates of analysis differences, some buoy data were withheld for independent verification. To attempt to make the selection random, we simply excluded any buoy data (both moored and drifting) with an ID ending in either 4 or 9. These buoys were excluded from all analyses including the bias correction step. This randomly excludes approximately 20% of the buoy data. The fraction of withheld buoys was selected to exclude enough data for verification while minimizing the impact on the analysis. An additional research buoy was obtained that was not available to the analyses and was also used as independent data. This buoy is located off the coast of Peru (20.1°S, 85.1°W) in a region with persistent cloud cover with little other in situ data. Thus, comparison of the analyses with this buoy should emphasize the advantage of microwave SST retrievals over IR. A technical report on this buoy is given by Lucas et al. (2001); information on the meteorological instrument package, including SSTs, is described by Hosom et al. (1995).

The six versions of the OI were run weekly from 10 December 1997 to 1 January 2003 where the date designates the day at the center of the week, Wednesday.

Table 1 lists the six versions of the OI along with difference statistics, which are discussed later.

4. Results

We now analyze the differences among our different datasets and products. First we show the coverage of the original four satellite input datasets: daytime and nighttime TMI and AVHRR. As mentioned in the previous section, we combined all TMI data into one average product. However, we originally separated TMI into day and night categories and it is useful to see the result. To compute the coverage, we first counted the number of the OI 1° ocean boxes that had at least one satellite observation per week between 40°S and 40°N. The ocean boxes include open ocean regions as well as coastal regions. The coverage was computed along each 1° latitude grid line as a percentage of ocean boxes with data relative to the total number of ocean boxes. Between 40°S and 40°N the total number of ocean boxes ranged between 206 and 348.

The weekly coverage is shown in Fig. 1. The AVHRR daytime coverage shows a persistent drop in coverage near the equator due to screening of clouds from the intertropical convergence zone (ITCZ). In addition, there is a seasonal drop in daytime AVHRR retrievals to 0% in middle latitudes during winter. This is due to the changes in the orbit of *NOAA-14*. *NOAA-14*'s equatorial crossing changed from the planned value of roughly 1400 to as late as 1800 local time as the orbit aged. This limited the number of daytime retrievals in the winter hemisphere at middle and high latitudes because of the sun's zenith angle. *NOAA-14* was the operational platform for AVHRR through February 2001; *NOAA-16* became the operational platform for AVHRR in March 2001. The operational replacement of *NOAA-14* by *NOAA-16* ended this type of data loss. The nighttime AVHRR coverage shows a reduced impact of ITCZ clouds compared to the daytime AVHRR coverage. This is not due to a diurnal signal but due to different daytime and nighttime cloud-screening algorithms. A clear seasonal cycle is evident in both the daytime and nighttime

TABLE 1. The rmsd's of the *average* weekly buoy minus OI difference. There are three OI analyses with satellite bias correction (labeled Yes) and three OI analyses without bias correction (labeled No). The results are divided into three buoy categories: drifting, moored, and all. The rmsd's are computed for all weeks from 10 Dec 1997 to 1 Jan 2003. Only buoy observations between 35°S and 35°N are used. Bold type indicates the lowest rmsd's for each category of buoy for the three OI analyses with and three analyses without bias correction. The number of differences is the same for all buoy categories and equal to the number of weeks, 265. The moored buoy off the coast of Peru (25.1°S, 85.1°W) is not included in these results.

OI analysis	Satellite bias correction	Drifting buoy rmsd	Moored buoy rmsd	All buoy rmsd
AVHRR only	Yes	0.085	0.123	0.080
TMI only	Yes	0.089	0.130	0.085
TMI + AVHRR	Yes	0.089	0.122	0.082
AVHRR only	No	0.191	0.152	0.181
TMI only	No	0.134	0.192	0.135
TMI + AVHRR	No	0.092	0.126	0.087

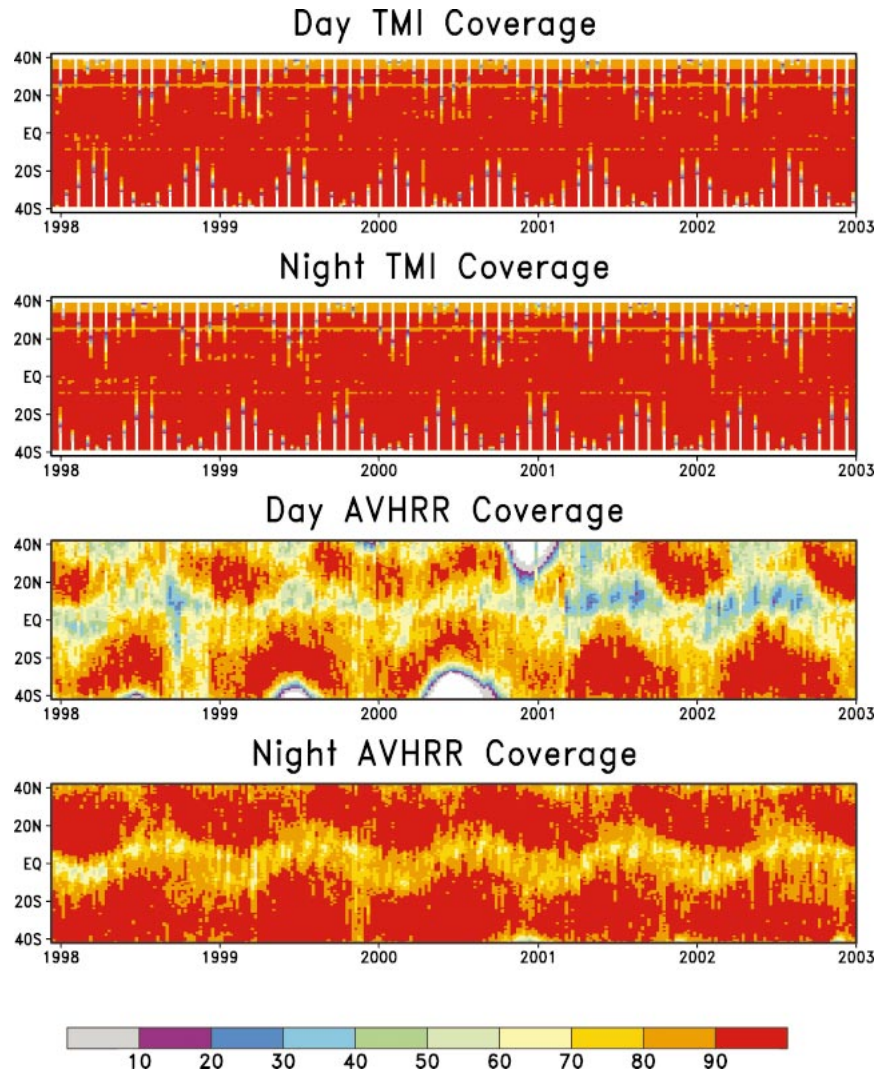


FIG. 1. Percentage of the number of weekly 1° ocean boxes with satellite data along each 1° latitude line. (top to bottom) Satellite data are daytime TMI, nighttime TMI, daytime AVHRR, nighttime AVHRR; 0% is shown as white to indicate missing values. The period of record is 10 Dec 1997 to 1 Jan 2003.

AVHRR cloud cover. Although the nighttime AVHRR coverage does not show any clear impact in the change from *NOAA-14* to *NOAA-16*, the change did affect the SSTs as will be discussed.

Figure 1 shows that TMI coverage periodically has regions south of 20°S and north of 20°N where the daytime and nighttime sampling drops to 0% (missing). The coverage is related to the precession of the TMI orbit. If limited sampling is available during the day, then good sampling is available at night, and the inverse. Thus, the combined day and night coverage would always appear complete as shown in Stammer et al. (2003). However, it should be noted that the average crossing time at any location would vary by time. Closer examination of the TMI coverage shows persistent horizontal lines where coverage drops because TMI must

exclude retrievals near land to avoid large biases from land contamination. In addition, there was a drop in TMI retrievals during the week of 15 August 2001 when the TMI orbit was changed, which is not evident here. This resulted in very limited amount or a complete loss of TMI data from 13–17 August. The orbit change required a recalibration of the TMI algorithms. Until this was done, the old algorithm produced inaccurate TMI retrievals.

The impact of the TMI orbit precession on weekly daytime and nighttime averages can be seen in Fig. 2. This figure shows the daytime and nighttime TMI weekly anomalies for the week of 10 January 2001 on the original 0.25° grid available from Remote Sensing Systems. The spatial scales for the figure and the selected week were chosen because of large TMI nighttime dif-

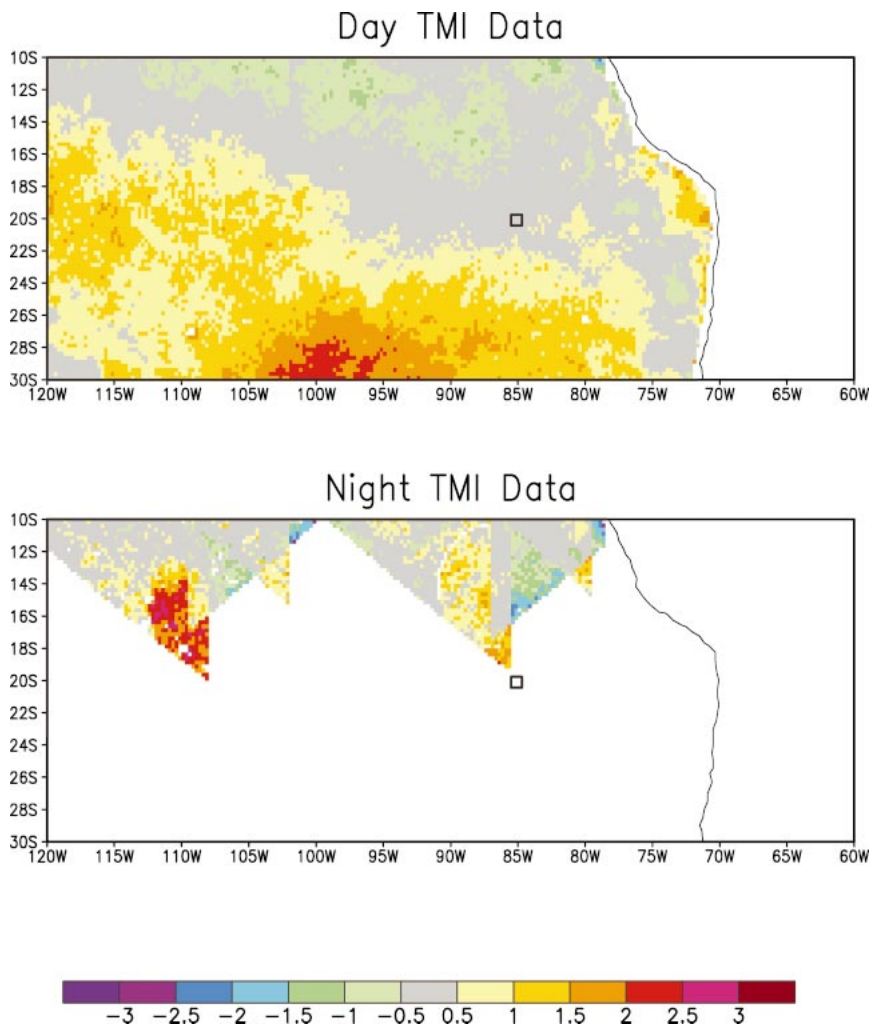


FIG. 2. (top) Daytime and (bottom) nighttime TMI SST anomalies ($^{\circ}\text{C}$) on 0.25° grid for the week of 10 Jan 2001. The location of the moored buoy off the coast of Peru (25.1°S , 85.1°W) is indicated by the box.

ferences with respect to the moored research buoy off the coast of Peru. The figure shows a relatively smooth daytime pattern along with a noisy nighttime pattern with very limited coverage south of 10°S . Even in regions with nighttime coverage, the number of nighttime observations is much lower than the number of daytime observations. Thus, any analysis with roughly equal weighting of these daytime and nighttime patterns could produce analysis problems because of sampling. At this latitude, sampling problems with either daytime or nighttime data would occur roughly every 4 to 5 weeks. However, once the TMI data are computed by the average of the combined daytime and nighttime observations, the resulting fields are less noisy. For the week shown in Fig. 2, the final field very closely resembles the daytime field. Because of this sampling problem, we have used combined daytime and nighttime averages as TMI input to the OI. We have shown the result in Fig. 2 to explain why we used a combined product in

the OI and to emphasize that the average TMI crossing time must vary by week. Of course combining day and night retrievals could produce bias aliases if a diurnal signal is present.

We now show the weekly time series for each satellite SST anomaly averaged between 30°S and 30°N at the top of Fig. 3. These curves are derived directly from the satellite data without *any* OI analysis processing. The results show an overall agreement between daytime AVHRR and TMI throughout the period. However, there are large differences between the daytime AVHRR and TMI in early 2001 and early 2002. The nighttime AVHRR shows the largest differences compared to the other products. Throughout our period of interest, the nighttime AVHRR is roughly 0.2°C cooler than the other two products prior to October 2000. From October 2000 to February 2001, the nighttime AVHRR becomes roughly 0.5°C cooler than the other products. After February 2001, the negative differences compared to the

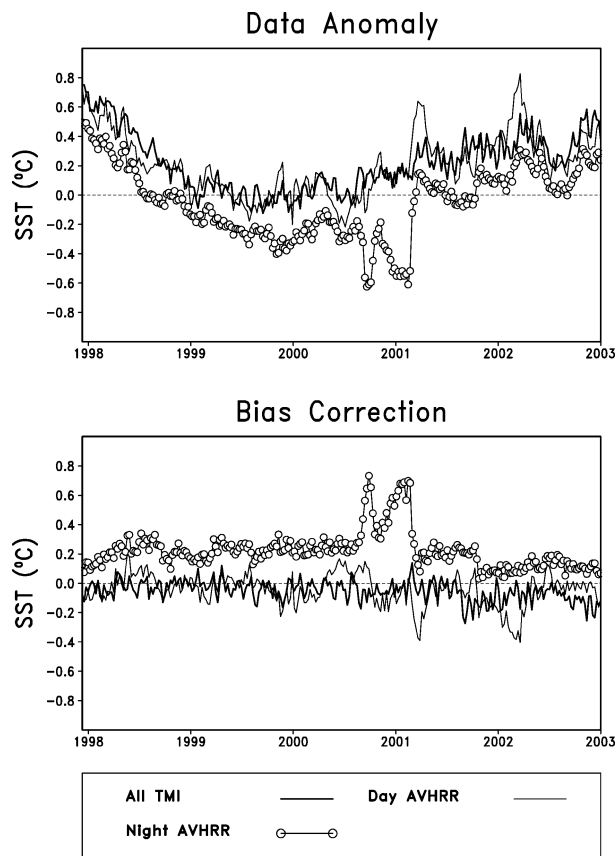


FIG. 3. Time series of weekly daytime and nighttime TMI and AVHRR average (30°S – 30°N) SSTs from 10 Dec 1997 to 1 Jan 2003. (top) SST anomalies; (bottom) the correction added to satellite data before it is used in the bias-corrected OI analyses.

other products are reduced to about half the magnitudes that they were prior to October 2000. The differences in the October 2000 to February 2001 period for nighttime AVHRR occurred at the end of the useful lifetime for *NOAA-14*. D. May (2003, personal communication) reported that *NOAA-14* nighttime accuracy became highly variable at the end of 2000 due to an onboard sensor anomaly. The source of the problem was due to a combination of solar radiation on the instrument with the resultant thermal emission from onboard objects. These effects occurred as the spacecraft moved out of the shadow of the earth at a low sun-elevation angle.

In the Poisson bias correction step, a spatially smoothed satellite correction is computed relative to in situ data. This correction is added to the satellite data before the data are used in the OI. The 30°S – 30°N average of the time series of the correction is shown at the bottom of Fig. 3. Here we see similar results to those at the top of the figure. However, now we have in situ data to determine which differences among satellite products were actually biases. The results show that the strongest corrections were needed for the nighttime AVHRR. As can be anticipated from the top of Fig. 3

a strong positive correction of roughly 0.5°C is needed from October 2000 to February 2001. Also we can see that a negative correction of roughly 0.2° – 0.3°C is needed for the daytime AVHRR for two periods in early 2001 and 2002. We also see that TMI usually requires a small negative correction, while AVHRR daytime is more variable than TMI and requires corrections of opposite signs over our period of interest.

The temporally averaged spatial fields associated with bias correction for each satellite source are shown in Fig. 4 for the period 10 December 1997 to 1 January 2003. The TMI bias corrections are of mixed signs with the largest positive correction north of 30°N in the Pacific. The most extensive negative correction is roughly in the region of the South Pacific convergence zone (SPCZ). The daytime AVHRR bias corrections are smaller than TMI but in somewhat the same areas. The largest corrections, as expected, occur for the nighttime AVHRR. These corrections are overall positive and occur in the tropical and midlatitude North Atlantic, the tropical Indian, and the midlatitude North and South Pacific Oceans. During the October 2000 to February 2001 period, all corrections were of similar spatial scales as shown in the figure but of larger magnitudes.

The need for positive bias corrections in TMI and AVHRR north of 30°N in the Pacific could indicate an in situ data problem, because the TMI and AVHRR error characteristics are not the same. In this region, the set of in situ data are dominated by SSTs from ships. Reynolds et al. (2002) examined the differences between collocated ship and buoy data for a 1982–2000 period between 20° and 60°N and found a seasonal-dependent bias of the ship data with respect to the buoy data that ranged between 0.27° and 0.11°C . Thus, the bias correction needed for both TMI and AVHRR in the North Pacific may be due to the high density of ship-to-buoy data there. However, it is difficult to pursue this problem because bias corrections using buoy data alone are not accurate in this region because open ocean buoy data are sparse.

To examine how biases affect the OI analysis, we show in Fig. 5 the 30°S to 30°N averaged time series of the weekly OI SST anomaly for our three versions: AVHRR only, TMI only, and TMI + AVHRR. The top of Fig. 5 shows these analyses without satellite bias correction, the bottom with correction. The analyses without bias correction diverge because of biases in the satellite data. In particular the biases in nighttime AVHRR data between October 2000 and February 2001 strongly impact the anomalies in the AVHRR-only OI. The TMI + AVHRR OI shows a reduced impact of the nighttime AVHRR biases. The top of Fig. 5 shows that the three OI versions with bias corrections are almost identical. The large-scale bias correction has worked as designed to remove large-scale satellite bases. As discussed later, a penalty for the bias correction is that additional noise is added to the analysis.

We now examine the zonal cross sections of the OI

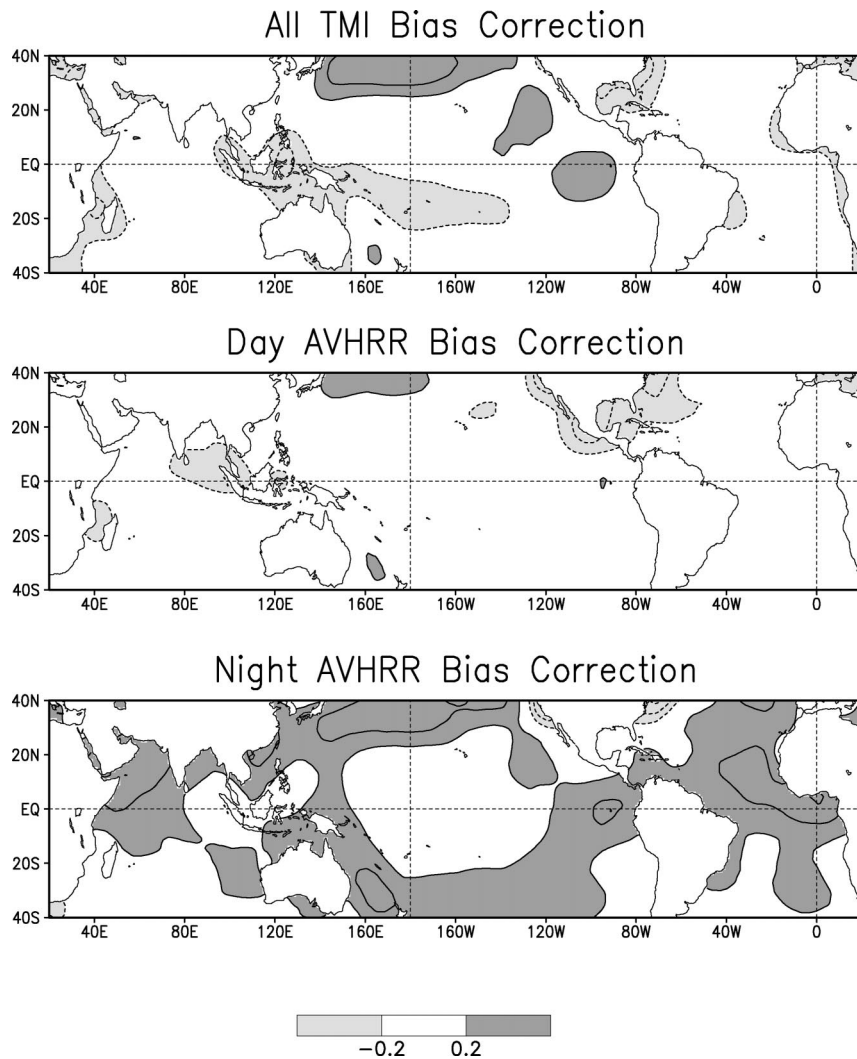


FIG. 4. Temporal average (10 Dec 1997 to 1 Jan 2003) of the corrections ($^{\circ}\text{C}$) added to the satellite data before they are used in the bias-corrected OI analyses. (top to bottom) The TMI, the daytime AVHRR, and the nighttime AVHRR corrections. The contour interval is 0.1°C ; there is no 0°C contour.

anomalies with time in Fig. 6. The three patterns for the OI with bias correction are very similar as suggested by the time series in the bottom of Fig. 5. Thus, we show all three versions of the OI without the bias correction along with only one version of the OI with bias correction: the TMI + AVHRR version. The bias-corrected OI shows the near-equatorial signature of the strong 1997/98 El Niño (positive SST anomalies), followed by a weak La Niña from the middle of 1998 to the end of 2000 (weak negative anomalies). This is followed by a weak El Niño period that begins to strengthen toward the end of our period of record. North of 20°N and south of 20°S , the anomalies are generally positive for the entire period shown. The OI analysis without bias correction using TMI only is generally very similar to the bias-corrected OI, except for some week-to-week noise, which may be due to the change in the

time of day of the observations due to the orbit precession. The OI analysis without bias correction using AVHRR only does not show the week-to-week noise. However, biases are evident relative to the OI bias-corrected versions especially in the October 2000 and February 2001 period as expected from the top of Fig. 5. The OI analysis without bias correction using TMI + AVHRR is truly a blend of the TMI-only and AVHRR-only analyses. The use of both types of satellite anomalies reduces the TMI week-to-week noise and reduces the effect of the AVHRR nighttime biases.

To examine the relatively small differences between the bias-corrected TMI-only and AVHRR-only OI analyses, we show the average difference for 10 December 1997 to 1 January 2003 at the top and the rms difference (rmsd) at the bottom of Fig. 7. The rmsd is the more useful because it includes both bias and variability.

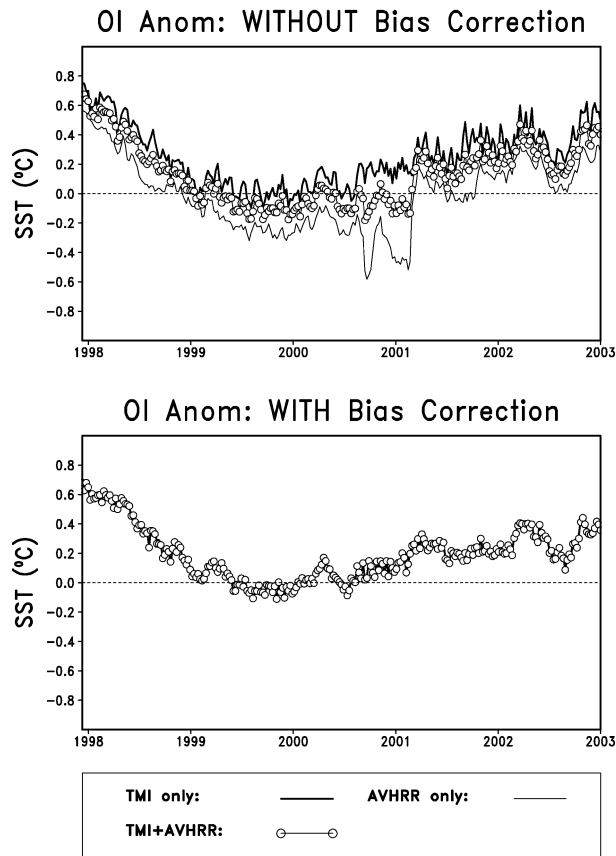


FIG. 5. Time series of OI SST (average, 30°S – 30°N) weekly anomalies using AVHRR-only, TMI-only, and TMI + AVHRR data from 10 Dec 1997 to 1 Jan 2003. (top) The OI analyses without satellite bias correction; (bottom) the OI analysis with satellite bias correction.

However, the average difference allows the sign of the bias to be determined. The rmsd results show small increasing differences near islands, north of 30°N and south of 30°S , along the coastlines of most continents, and along the equator. Please recall that biases have already been corrected on large spatial scales (roughly 10° and greater). Reynolds et al. (2002) found that the bias correction method eliminated most of the bias in AVHRR but tended to leave residuals. Thus, some of the differences may be due to satellite bias problems such as biases due to cloud and aerosol contamination in AVHRR data and land contamination in TMI data. They may also be due to ocean variability, which is poorly resolved by the OI. The differences north of 35°N and south of 35°S are near the limits of TMI retrievals and may be a problem with the TMI algorithm.

We now use the withheld buoy data to help quantify these results. Figure 8 shows the distribution of the moored (top of figure) and drifting (bottom) buoys that can be used as independent data. To simplify the display in Fig. 8, we only show buoys that had observations for at least 150 of the 265 weeks possible. Drifting buoys tend to move large distances over this period and the

SSTs from drifters would be difficult to use to determine the regional differences shown in Fig. 7. This problem is exacerbated because buoy IDs are reused after buoy failure. Thus, for example, the ID for the drifting buoy that traveled roughly along 5°N in the central tropical Pacific was reused for a buoy in the South Pacific near 20°S . Thus, moored buoys are better for focusing on regional differences. However, drifting buoys may be more useful than moored buoys for overall differences because they sample more regions.

Figure 9 shows the time series of the smoothed weekly average OI analysis SSTs minus collocated buoy SSTs between 35°S and 35°N . All independent drifting and moored buoys are used with the exception of the moored buoy off the coast of Peru. The top of Fig. 9 shows the difference without bias correction; the bottom shows the difference with bias correction. The top part shows that the TMI + AVHRR OI analysis without bias correction tends to have a reduced bias comparable to the other two analyses. This is because the causes of errors in microwave and IR instruments are independent and may tend to cancel. The lower part of Fig. 9 shows that the bias correction results are very similar for all analyses on these large scales. Note that a residual positive bias of roughly 0.05°C remains in the OI even with bias correction. In fact the overall bias relative to the withheld data does not necessarily improve with bias correction as is shown during 1988 in the case of the combined TMI + AVHRR analyses. However, the bias correction does reduce the OI bias for the TMI-only and AVHRR-only analyses. Although the overall TMI and AVHRR biases are of opposite signs and tend to cancel in the combined product, this may not always be the case. Furthermore, as shown in Fig. 4, regional differences exist that do not cancel. Thus, bias correction of both TMI and AVHRR is necessary.

To show a summary of the biases, we computed the rmsds of the average weekly buoy minus collocated OI difference in Table 1. This method of computing the average weekly difference smooths some of the individual differences that may be due to noise in the analyses (including the bias corrections) and the buoy data. Here we see that the rmsds are very similar for all OI analyses with bias corrections. The table also shows that the rmsd values for all OI analyses without bias correction are worse than the values with bias correction. In addition, for the analyses without bias correction, the TMI + AVHRR OI analysis is clearly better than the other two versions without bias correction. Comparison of the TMI-only and AVHRR-only OI analyses without bias correction show that the rmsds are lower for the TMI-only analysis than for the AVHRR-only analysis except for the comparison with moored buoys. This difference in moored buoys is due to larger TMI differences with respect to the coastal moored buoys in the Atlantic and Gulf of Mexico. Again, as noted earlier, the two combined TMI + AVHRR OI versions are similar and the version without bias correction is successful

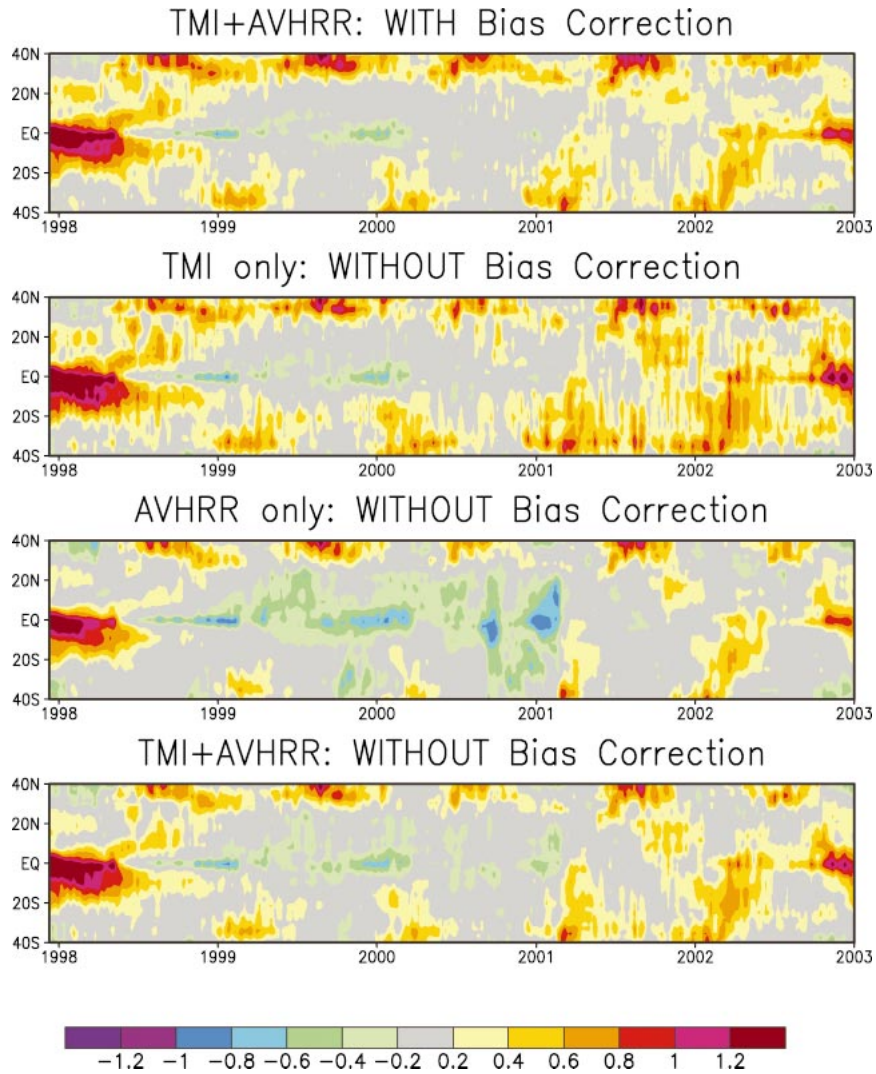


FIG. 6. Zonal average cross section of the OI SST weekly anomalies ($^{\circ}\text{C}$). (top to bottom) The analyses shown are TMI + AVHRR with bias correction, TMI only without bias correction, AVHRR only without bias correction, and TMI + AVHRR without bias correction. The period of record is 10 Dec 1997 to 1 Jan 2003.

because the overall TMI and AVHRR biases are of opposite signs.

We have examined the differences for each moored buoy. Other than the difference between the coastal buoys mentioned previously, the results at each buoy were too variable to make any overall conclusions. Thus we now focus on the OI differences with respect to the moored buoy off the coast of Peru (25.1°S , 85.1°W). Because this buoy uses two quality-controlled Improved Meteorology (IMET) instrument packages (Hosom et al. 1995), which are calibrated before and after deployment, we believe the buoy's SSTs are very reliable. There are several other advantages for using this buoy. The first is that the buoy's SSTs were not used to calibrate or verify the AVHRR or TMI algorithms. The second is that this region tends to have persistent cloud

cover, which should give the TMI product a clear advantage. The third is that Fig. 7 indicates that this location has important differences between AVHRR-only and TMI-only OI analyses with bias correction.

The weekly OI minus buoy difference at 25.1°S , 85.1°W is shown in Fig. 10 without smoothing. The time series begins in the week of 11 October 2000 when the buoy was first deployed. Because the time series are relatively noisy, we do not show time series of the TMI + AVHRR analyses for clarity. However, we summarize the results for all analyses later. The time series at the top of Fig. 10 (OI without bias correction) show that the AVHRR-only analysis tends to have a negative bias at the beginning of the time series (before March 2001) when *NOAA-14* was failing (see Fig. 3). The TMI-only analysis shows several positive spikes during the April

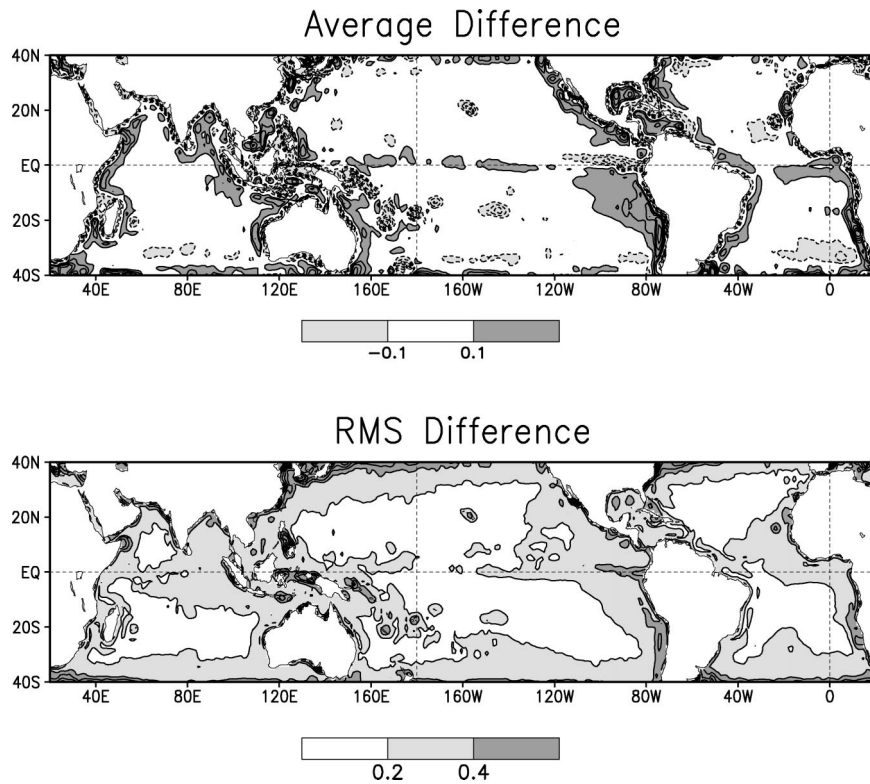


FIG. 7. Temporal average (10 Dec 1997 to 1 Jan 2003) of the difference ($^{\circ}\text{C}$) between the TMI-only and AVHRR-only bias-corrected OI analyses. (top) The average difference; (bottom) the rms difference. The contour interval is (top) 0.1° and (bottom) 0.2°C . The 0°C contour is not shown.

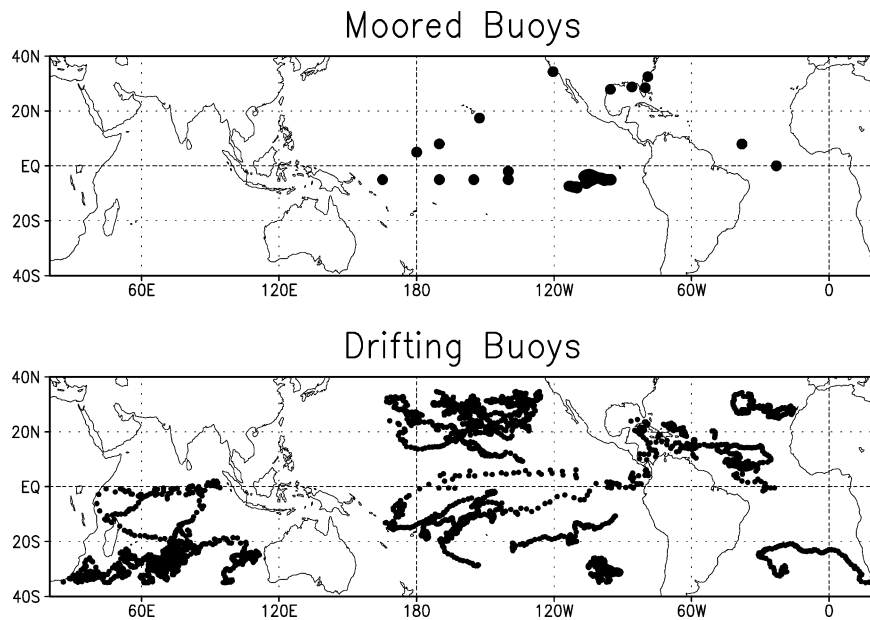


FIG. 8. Distribution of the withheld buoys that are used for independent verification. Only buoys that had data for at least 150 of the 265 weeks are shown. (top) The moored buoys; (bottom) the drifting buoys. The moored buoy off the coast of Peru had only 117 weeks of data and is not shown.

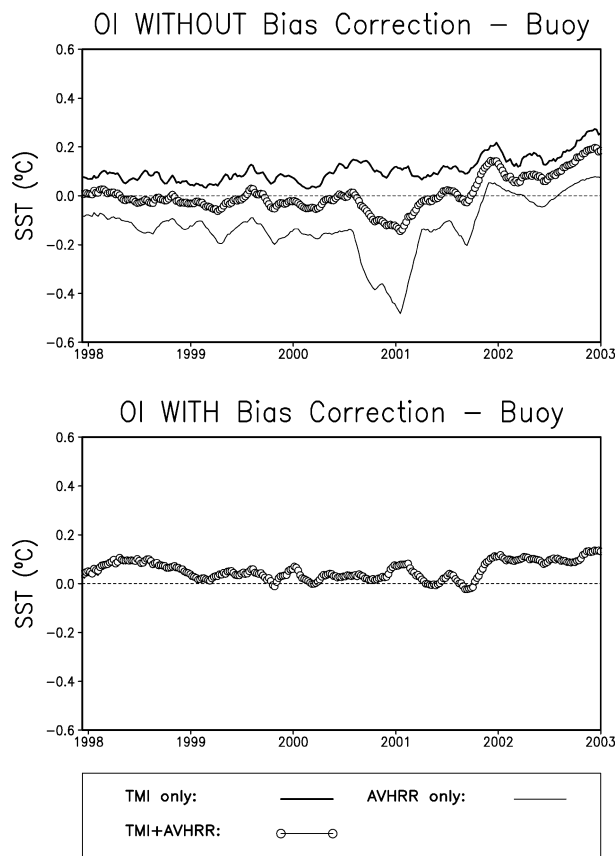


FIG. 9. Time series of weekly OI analysis minus buoy average differences for 10 Dec 1997 to 1 Jan 2003. All independent drifting and moored buoys are used except the moored buoy off the coast of Peru. Differences with respect to OI analysis (top) without bias correction; (bottom) with bias correction. Three OI analyses: AVHRR only, TMI only, and TMI + AVHRR. All time series have been smoothed over 11 weeks by a boxcar average.

to October period in 2001. The largest was during the week of 15 August 2001 when the TMI orbit was changed and several days of data were lost. The bottom of Fig. 10 shows the time series of the difference between the analyses and the buoy for the OI analyses with bias correction. Here the initial negative bias in AVHRR is corrected along with the positive TMI spikes in 2001. After October 2001, all time series look similar and there is no clear advantage for satellite bias correction at this location. Some of the differences between the analysis and the buoy SSTs are due to the difference between a point measurement and a smoothed analysis. It would have been useful if several buoys were available in this region.

We next examine the overall rmsds of the biases in Table 2. These results show a group of three analyses that have similar rmsd values: the OI TMI + AVHRR analyses with and without bias correction and the AVHRR-only analysis with bias correction. The next group has two analyses, the OI TMI-only analyses with and without bias corrections, with slightly large rmsds.

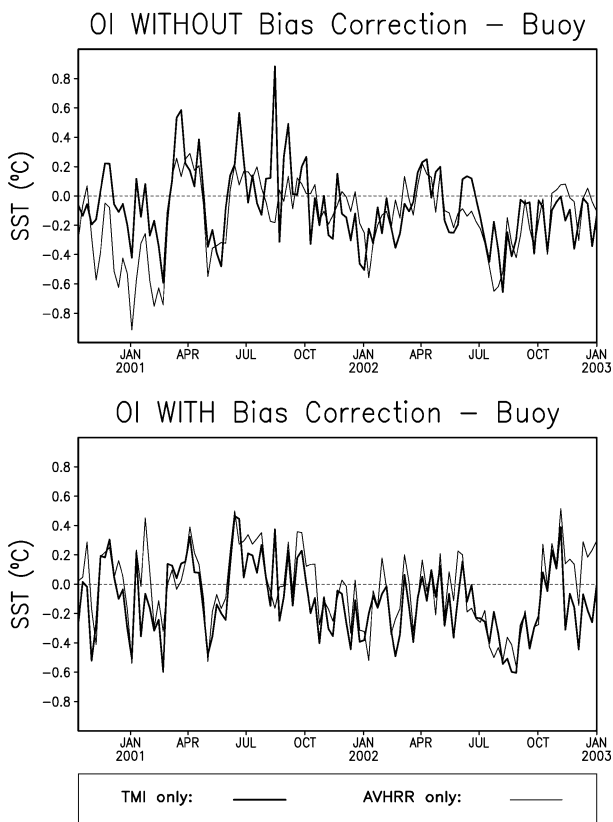


FIG. 10. Time series of weekly OI analysis minus the moored buoy off the coast of Peru (25.1°S, 85.1°W) for 11 Oct 2000 to 1 Jan 2003. Two OI analyses: AVHRR only, and TMI only. The time series have not been smoothed. Differences with respect to OI analysis (top) without bias correction; (bottom) with bias correction.

However, the remaining AVHRR-only analysis without bias correction is clearly the worst, with the largest rmsd. It is interesting to point out that the original OI TMI-only analysis without bias correction with separated day and night TMI data had an even larger rmsd value of 0.330°C. Thus, our decision to not separate day and night TMI data is clearly justified.

To better quantify the change in the analyses in time,

TABLE 2. The rmsd's of the weekly buoy minus OI difference for the moored buoy off the coast of Peru (25.1°S, 85.1°W). There are three OI analyses with satellite bias correction (labeled Yes) and three OI analyses without bias correction (labeled No). The rmsd's are computed for all weeks from 11 Oct 2000 to 1 Jan 2003. Bold type indicates the lowest rmsd's for each category for the three OI analyses with and three analyses without bias correction.

OI analysis	Satellite bias correction	OI - buoy rmsd
AVHRR only	Yes	0.255
TMI only	Yes	0.266
TMI + AVHRR	Yes	0.250
AVHRR only	No	0.288
TMI only	No	0.262
TMI + AVHRR	No	0.254

we computed the lag-1 autocorrelations of the OI weekly SST anomalies for the entire data period (10 December 1997 to 1 January 2003). Analyses where SST patterns persist in time will have higher autocorrelations while noisy analyses will have lower correlations. As discussed in Reynolds and Smith (1994), the bias corrections are done using the weekly in situ observations as fixed internal and external boundary points, while the satellite bias correction is determined by solving Poisson's equation forced by the Laplacian of the satellite data. The bias correction is then added to the satellite data before it is used in the OI. Because the in situ data vary spatially with time, the internal boundary conditions also vary with time. Especially in data-sparse regions, this can add noise to the bias correction and could make the OI with bias correction noisier than the OI without bias correction.

Comparison of the autocorrelations for the six OI analyses showed there were almost no differences in the bias-corrected analyses. Thus, we again show all OI analyses without bias correction while showing only one version of the OI with bias correction, the version using TMI + AVHRR. The results for analyses without bias corrections (Fig. 11) show that the autocorrelations are highest for the AVHRR-only version and lowest for the TMI-only version. This difference is due to the week-to-week noise in TMI as expected from Fig. 6. The autocorrelation for the OI analysis without bias correction using TMI + AVHRR lies between the other two OI analyses without bias correction.

It is important to note that the OI TMI + AVHRR version *with* bias correction has a lower autocorrelation than the OI TMI + AVHRR *without* bias correction. Thus, as expected, the satellite bias correction procedure adds noise. It would be better if satellite data did not require bias correction. Unfortunately, as we have shown, corrections are needed to minimize biases for climate-scale analyses.

5. Conclusions

Our results have shown that there are biases in the three satellite datasets considered here: TMI and daytime and nighttime AVHRR. Because global surface (land plus ocean) temperature warming trends are roughly $0.15^{\circ}\text{C decade}^{-1}$ over the last two decades (Folland et al. 2001), the differences shown in Fig. 3 are not negligible and must be corrected. Overall biases in the OI analyses without bias correction are clearly shown at the top of Fig. 9. Because the TMI and AVHRR biases are of opposite signs, the combined TMI + AVHRR analysis without bias correction has a reduced bias compared to the TMI-only or AVHRR-only analyses without bias correction. However, this reduction was because the overall biases of TMI and AVHRR data are of opposite signs and this may be only fortuitous. On smaller spatial scales, as shown in Fig. 4 in parts of the eastern Pacific and midlatitude North Pacific, TMI

and AVHRR biases do not necessarily cancel. Thus, it is necessary to correct these biases even though some noise is added to the analyses by the correction step as shown in Fig. 11.

We have held back 20% of the in situ buoys from the OI analysis to use as independent data. In the comparisons, the OI analysis using AVHRR only, TMI only, and TMI + AVHRR showed that the bias corrections in the OI are very robust (see bottom portions of Figs. 5 and 9). Using the withheld buoy data, we could not prove that the combined TMI + AVHRR OI analysis with bias correction was better than the AVHRR-only OI analysis with bias. However, examination of Fig. 8 shows that the tropical coverage of the withheld data is not complete. In addition, the ship and the remaining 80% of the buoy data that were used in the bias correction sample the same regions, but more completely. Thus, any large-scale bias may already be corrected.

The advantage of TMI data is clearly shown in the OI analyses without bias correction. Because IR and microwave satellite algorithms are affected by different sources of error, biases may be reduced when both TMI and AVHRR data are used in the OI. This is clearly evident in the top portions of Figs. 5 and 9 and also evident in the intercomparisons with the buoy off the coast of Peru in Fig. 10. Clearly we cannot make a bias correction in regions where we have no in situ data. In these regions, the results of the analyses without bias corrections apply. In addition (see Fig. 1) TMI data can ensure satellite sampling in cloud-covered regions. Thus, TMI should be used along with AVHRR in the OI analyses. We believe that the use of more than one satellite product is helpful in diagnosing problems in any satellite product.

Our purpose in this paper was not so much to show that one satellite product was superior to another as it was to demonstrate that satellites can have unexpected problems that cause biases. The biases can occur from orbit changes, satellite instrument changes, and changes in physical assumptions on the physics of the atmosphere (e.g., through the addition of volcanic aerosols). Please recall that satellite instruments, even if perfect today, may fail in the future as the instrument ages. Thus, SST analyses that are designed to use in situ data to bias-correct satellite data and are designed to use different satellite products would be best protected from these changes. The OI analysis was designed in a period when only one satellite instrument was available. Because of the results from this study, we plan to continue to expand the number of satellite instruments used in the OI. In addition, we plan to reevaluate the OI analysis spatial error correlation scales. We believe that these scales can be reduced, at least over the last 5 yr, to allow the analysis to show more detail without greatly increasing the analysis noise.

It is an interesting and exciting time for SST analysis because new satellite instruments are now available and more will be available soon. [For example, the Ad-

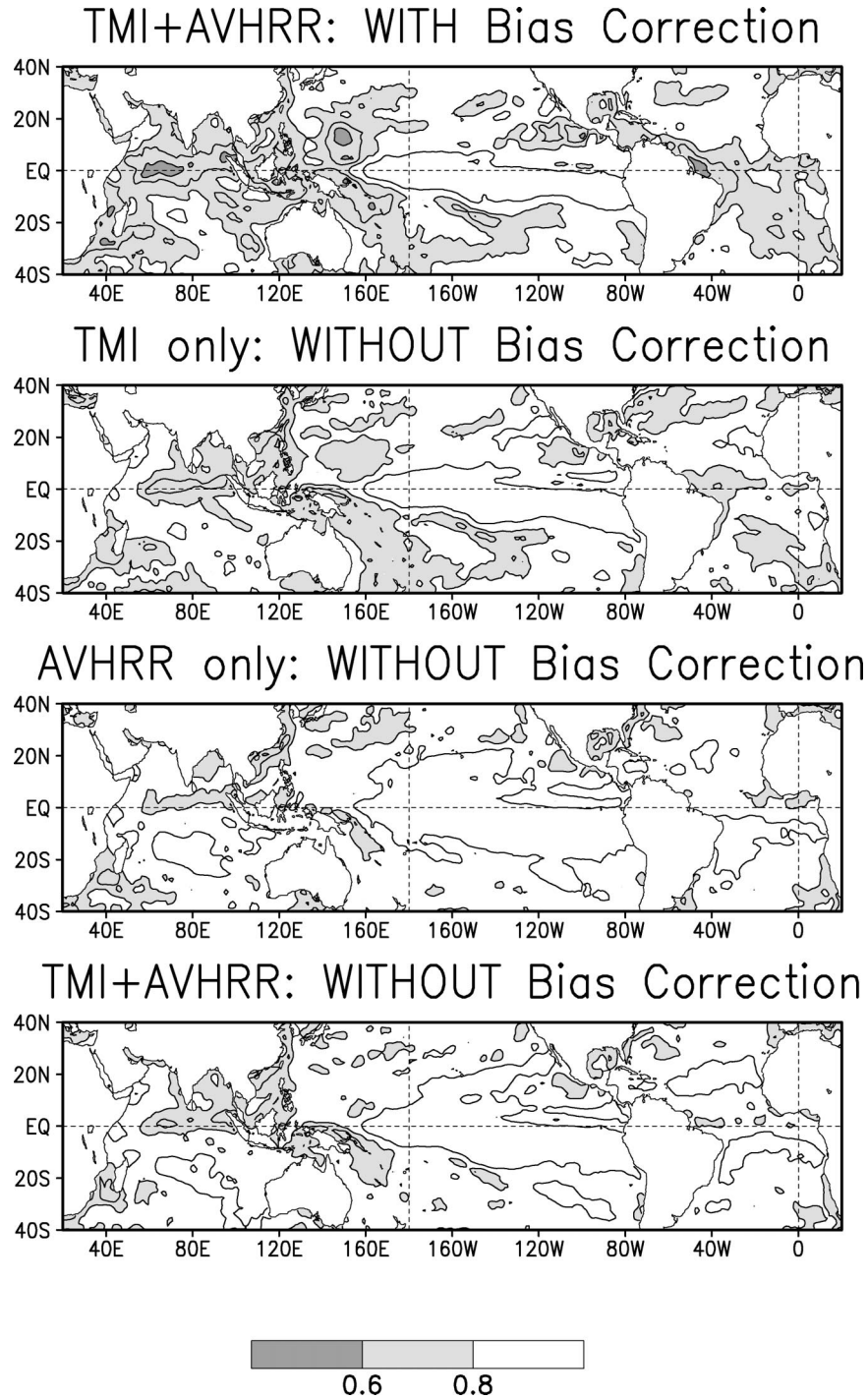


FIG. 11. Lag-1 autocorrelations for OI analyses for 10 Dec 1997 to 1 Jan 2003. (top to bottom) Analyses are TMI + AVHRR with bias correction, TMI only without bias correction, AVHRR only without bias correction, and TMI + AVHRR without bias correction. The contours are 0.6, 0.7, 0.8, and 0.9.

vanced Microwave Scanning Radiometer (AMSR), which was launched in June 2002, is now available with global coverage.] However, it is difficult for the user to sort out the advantages and disadvantage of each type

of satellite data. The problems we have discussed here will become even more difficult at higher spatial and temporal resolutions. In particular, the bias corrections done here are based on limited in situ data and such

corrections are much more difficult for analyses with higher spatial and temporal resolutions.

Analyses on high-resolution scales are being developed by many groups, including the Global Ocean Data Assimilation Experiment (GODAE) High-Resolution Sea Surface Temperature Pilot Project (GHRSSST-PP; see <http://www.ghrsst-pp.org>; Donlon et al. 2002). In this project, analyses are planned on roughly 10-km spatial scales with models of the diurnal cycle to correct for any diurnal signals and for the depth of the observation from the surface. One of the big advantages of this project is that all satellite data will be hosted at one site. Although a direct bias correction using in situ data is difficult, several diagnostic products will be computed to assure that the input satellite data are as accurate as possible. These diagnostics include time series such as those shown in Fig. 3. Our results show that monitoring satellite data are critical because satellite biases and other errors change with time. It is important for all users to know when any satellite errors have occurred and to have access to the metadata for each satellite instrument. If this is not done, it will be difficult to improve the accuracy of SST analyses.

Acknowledgments. We are grateful to NCDC and the NOAA Office of Global Programs, which provided partial support for this work. The graphics were computed using the Grid Analysis and Display System (GrADS; <http://grads.iges.org/grads>), Center for Ocean–Land–Atmosphere Studies. We are grateful to Dudley Chelton, Craig Donlon, Tom Smith, Diane Stokes, and Carissa Tartaglione for their comments on earlier drafts of this paper. We especially want to thank Bob Weller for suggesting the use of his IMET buoy off the coast of Peru. This buoy helped us to understand why TMI data should not be divided into separate daytime and nighttime categories.

REFERENCES

- Donlon, C. J., P. J. Minnett, C. Gentemann, T. J. Nightingale, I. J. Barton, B. Ward, and M. J. Murray, 2002: Toward improved validation of satellite sea surface temperature measurements for climate research. *J. Climate*, **15**, 353–369.
- Fairall, C. W., E. F. Bradley, J. S. Godfrey, G. A. Wick, J. B. Edson, and G. S. Young, 1996: Cool skin and warm layer effects on sea surface temperature. *J. Geophys. Res.*, **101**, 1295–1308.
- Folland, C. K., and Coauthors, 2001: Global temperature change and its uncertainties since 1861. *Geophys. Res. Lett.*, **28**, 2621–2624.
- Gandin, L. S., 1963: *Objective Analysis of Meteorological Fields* (in Russian). Gidrometeorizdat, 238 pp. (English translation by Israeli Program for Scientific Translations.)
- Hosom, D. S., R. A. Weller, R. E. Payne, and K. E. Prada, 1995: The IMET (Improved Meteorology) ship and buoy system. *J. Atmos. Oceanic Technol.*, **12**, 527–540.
- Kent, E. C., P. K. Taylor, B. S. Truscott, and J. A. Hopkins, 1993: The accuracy of voluntary observing ships' meteorological observations—Results of the VSOP-NA. *J. Atmos. Oceanic Technol.*, **10**, 591–608.
- , P. G. Challenor, and P. K. Taylor, 1999: A statistical determination of the random observational errors present in voluntary observing ships meteorological reports. *J. Atmos. Oceanic Technol.*, **16**, 905–914.
- Lorenc, A. C., 1981: A global three-dimensional multivariate statistical interpolation scheme. *Mon. Wea. Rev.*, **109**, 701–721.
- Lucas, L. E., and Coauthors, 2001: Long-term evolution and coupling of the boundary layers in the stratus deck regions of the eastern Pacific (STRATUS). Tech. Rep. WHOI-2001-04, UOP 2001-01, 94 pp. [Available from Upper Ocean Processes Group, Woods Hole Oceanographic Institution, Woods Hole, MA 02543.]
- May, D. A., M. M. Parmeter, D. S. Olszewski, and B. D. McKenzie, 1998: Operational processing of satellite sea surface temperature retrievals at the Naval Oceanographic Office. *Bull. Amer. Meteor. Soc.*, **79**, 397–407.
- McClain, E. P., W. G. Pichel, and C. C. Walton, 1985: Comparative performance of AVHRR-based multichannel sea surface temperatures. *J. Geophys. Res.*, **90**, 11 587–11 601.
- Reynolds, R. W., 1993: Impact of Mount Pinatubo aerosols on satellite-derived sea surface temperatures. *J. Climate*, **6**, 768–774.
- , and T. M. Smith, 1994: Improved global sea surface temperature analyses using optimum interpolation. *J. Climate*, **7**, 929–948.
- , C. K. Folland, and D. E. Parker, 1989: Biases in satellite derived sea-surface temperature data. *Nature*, **341**, 728–731.
- , D. E. Harrison, and D. C. Stokes, 2001: Specific contributions to the observing system, sea surface temperatures. *Observing the Ocean in the 21st Century*, C. J. Koblinsky and N. R. Smith, Eds., Bureau of Meteorology, 87–101. [Available from Bureau of Meteorology, GPO Box 1289K, Melbourne VIC 3001, Australia.]
- , N. A. Rayner, T. M. Smith, D. C. Stokes, and W. Wang, 2002: An improved in situ and satellite SST analysis for climate. *J. Climate*, **15**, 1609–1625.
- Stammer, D., F. Wentz, and C. Gentemann, 2003: Validation of microwave sea surface temperature measurements for climate purposes. *J. Climate*, **16**, 73–87.
- Wentz, F. J., and T. Meissner, 1999: AMSR ocean algorithm, version 2. RSS Tech. Rep. 121599A, 66 pp. [Available from Remote Sensing Systems, 438 First Street, Suite 200, Santa Rosa, CA 95401.]
- , P. D. Ashcroft, and C. L. Gentemann, 2001: Post-launch calibration of the TMI microwave radiometer. *IEEE Trans. Geosci. Remote Sens.*, **39**, 415–422.